

Tevatron Combination and Higgs Boson Properties

Weiming Yao^a

*Physics Division, Lawrence Berkeley National Laboratory,
One Cyclotron Road, Berkeley, CA 94720, USA*

We present the Tevatron combination of searches for the Higgs boson and studies of its properties. The searches use up to 10 fb^{-1} of Tevatron collider Run II data. We observe a significant excess of events in the mass range between 115 and 140 GeV/c^2 . The local significance corresponds to 3 Gaussian standard deviations at the mass of 125 GeV/c^2 . Furthermore, we separately combine searches for the Higgs boson decaying to $b\bar{b}$, $\tau^+\tau^-$, W^+W^- , and photon pairs in the final states. The observed signal strengths in all channels are consistent with the presence of a standard model scalar boson with a mass of 125 GeV/c^2 . Studies of the couplings at the Tevatron are consistent with SM predictions and are complementary to those performed at LHC.

1 Introduction

The standard model (SM) Higgs boson was first proposed in 1964 as the remnant of a scalar field (H) that could be responsible for the electroweak symmetry breaking¹. The quest for the Higgs boson particle, the last missing piece of the standard model, has been a major goal of particle physics and a central part of the Fermilab Tevatron collider physics program for several decades. Both CDF and D0 collaborations have finished their direct searches for the standard model Higgs boson using the complete Tevatron Run II dataset with an integrated luminosity of 10 fb^{-1} of proton-antiproton data. The results reported here are close to the final word on the Higgs studies at the Tevatron, which have been recently submitted for publication². The searches are performed for assumed Higgs masses between 90 and 200 GeV/c^2 .

In the standard model, the mass of the Higgs boson (m_H) is a free parameter and is indirectly constrained to be less than 152 GeV/c^2 at the 95% confidence level (CL)³ by the global fit of the electroweak precision data including the recent top-quark mass and W boson mass measurements from the Tevatron^{4,5}. The direct searches from LEP2⁶ set the limit of Higgs mass above 114.4 GeV/c^2 at the 95% CL. On fourth of July 2012, the ATLAS and CMS collaborations announced the observation of the Higgs-like particle^{7,8} with a mass of approximately 125 GeV/c^2 . Much of the power of the LHC searches comes from $gg \rightarrow H$ production and Higgs boson decays to $\gamma\gamma$, W^+W^- , and ZZ , which probes the couplings of the Higgs boson to other bosons. The Tevatron has recently reported a 3.1 sigma excess of $H \rightarrow b\bar{b}$ events in association with a vector boson production, which may provide the first evidence of Higgs coupling to b quarks⁹.

1.1 Higgs Search Strategies

The dominant Higgs boson production processes at the Tevatron are gluon-gluon fusion ($gg \rightarrow H$) and the associated production with a W or Z boson¹⁰. Figure 1 shows the Higgs boson

^aOn behalf of the CDF and D0 Collaborations

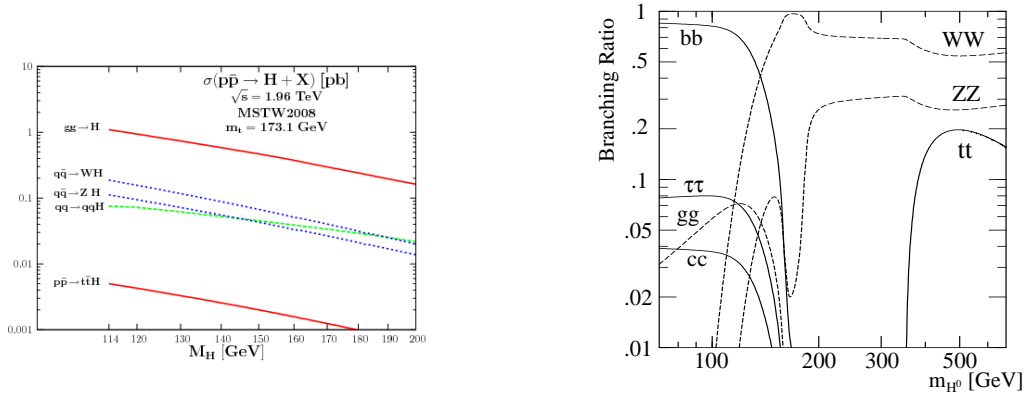


Figure 1: SM Higgs production cross sections at the Tevatron (left) and its decay branching ratio (right) as a function of the Higgs boson mass.

production cross sections at the Tevatron as a function of Higgs boson mass and the Higgs decay branching ratio in the standard model [11](#). The Higgs boson decay is dominated by $H \rightarrow b\bar{b}$ in the low-mass range ($m_H < 130 \text{ GeV}/c^2$) and by $H \rightarrow W^+W^-$ or ZZ^* in the high-mass range ($m_H > 130 \text{ GeV}/c^2$). A search for a low-mass Higgs boson in the $gg \rightarrow H \rightarrow b\bar{b}$ channel is extremely difficult because the $b\bar{b}$ QCD production cross section is many orders of magnitude higher than the Higgs production. Requiring the leptonic decay of the associated W or Z boson greatly improves the expected signal over background ratio in the $b\bar{b}$ channel, which makes it to be the most promising channel for the low-mass searches at the Tevatron. Other searches in the secondary channels for $H \rightarrow \gamma\gamma$, $\tau^+\tau^-$, and $t\bar{t}H$ are also considered. We have to combine all searches in many different channels in order to obtain the best sensitivity.

The difficulty for the Higgs search at the Tevatron is due to the fact that the Higgs signal is so small compared to other standard model processes with the same final states. Search strategies employed by CDF and D0 have been constantly improving over time. We first maximize the signal acceptances by using efficient triggers, excellent lepton identifications, and b -tagging. Then we use multivariate analysis (MVA) to exploit the kinematic differences between signal and background, which can further enhance the signal-to-background ratio from 1% up to the 10% level in the high score regions. The procedures are iterated with improvements for every major update until the best sensitivity is achieved.

Figure 2 shows the evolution of achieved and projected median expected upper limits on the SM Higgs boson cross section as a function of the luminosity used for the low-mass searches (left) and the high-mass searches (right). The solid lines are the luminosity projection assuming there is no further improvement available. In the past, we have constantly introduced and improved analysis techniques to gain sensitivity far beyond expectation from increased luminosity. The orange band corresponds to our conservative and aggressive projections based on 2007 summer results. The last update with full dataset indicates we have exceeded our most optimistic expectations.

1.2 CDF and D0 Searches

Event selections are similar in the CDF and D0 analyses, typically consisting of a preselection based on event topology and kinematics. Multivariate analysis (MVA) techniques are used to combine several discriminating variables into a single final discriminant that is used in the analysis. The gain of sensitivity from MVA is about 10-25%, compared to use a single best variable, such as the dijet mass. Each channel is then divided into exclusive sub-channels according to various lepton, jet multiplicity, and different b -tagging categories. This procedure groups events with similar signal-to-background ratio to optimize the overall sensitivity. For $H \rightarrow b\bar{b}$ signatures we look for a $b\bar{b}$ mass resonance in associated with a W or Z boson where the

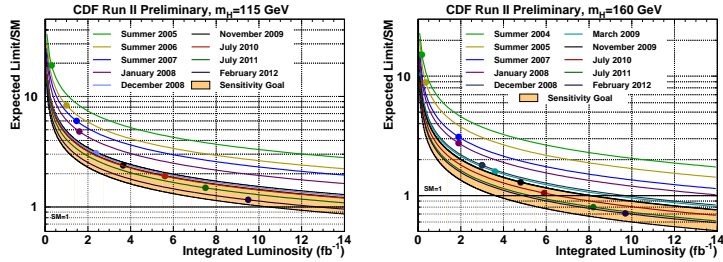


Figure 2: Achieved and projected median expected upper limits on the SM Higgs boson cross section for $m_H=115$ GeV/ c^2 (left) and 165 GeV/ c^2 (right) as a function of integrated luminosity used for each major update. The solid lines are $1/\sqrt{L}$ projections assuming no further improvements. The orange band corresponds to the Summer 2007 performance expected limit divided by 1.5 on top, and by an additional factor of 1.5 on bottom.

W decays into $l\nu$, the Z decays into l^+l^- , and $\nu\bar{\nu}$. The $WH \rightarrow l\nu b\bar{b}$ channel is the most sensitive channel and we apply b -tagging and use advanced multivariate analysis (MVA) to suppress the W +jets and top backgrounds.

For high mass Higgs signatures, we look for Higgs boson decaying into W^+W^- pair in the inclusive $gg \rightarrow H$ events that lead to many interesting final states. The most sensitive channel is both W decaying leptonically that gives an opposite-sign dilepton, a large missing transverse energy, and plus some jets in the final state. Due to the miss neutrinos, we can not reconstruct the Higgs mass and have to rely on the event kinematic that distinguishes signal from background. For example, the opening angle between two leptons in the signal events is generally smaller than that in background events due to the fact that the Higgs boson is a scalar particle. Furthermore, the missing energy of momentum is larger and the total transverse energy of the jets is lower than they are typically in background events. We combine all these variables into a single final discriminant, which improves the sensitivity significantly in the high-mass channel.

Although the primary sensitivity for $m_H < 130$ GeV/ c^2 is provided by the $H \rightarrow b\bar{b}$ analyses and for $m_H > 130$ GeV/ c^2 by the $H \rightarrow W^+W^-$ analyses, additional sensitivity is achieved by the inclusion of other channels. Both collaborations contribute analyses searching for Higgs boson decaying into tri-lepton final states, τ -lepton pairs, diphoton, and $t\bar{t}H$.

2 Combination Procedures

We combine searches in many channels with different production cross section and decay branching ratio, and set limits with respect to nominal SM prediction. We combine the results using a combined likelihood formed from a product of likelihoods for the individual channels. Systematic uncertainties are treated as nuisance parameters with truncated Gaussian. The common systematic between CDF and D0 are the luminosity, theoretical cross sections, and PDF uncertainties, which are treated as correlated. Other sources of systematic are experiment dependent, treated uncorrelated between experiments, but correlated within the experiment, such as lepton identification, b -tagging efficiency, jet-energy scale (JES), detector related efficiencies, and instrumented backgrounds. Most systematic parameters are constrained by the data in the background dominated regions.

In order to check the consistency between data and background, we rebin the final discriminant from each channel in terms of signal-to-background ratio (s/b) so that the data with similar s/b may be added without loss of sensitivity. The resulting data distributions before and after background subtraction are shown in Figure 3. There seems to be a small excess of Higgs boson candidate events in the highest s/b bins relative to the background-only expectations, and the excess seems consistent with the expected signal of $m_H = 125$ GeV/ c^2 .

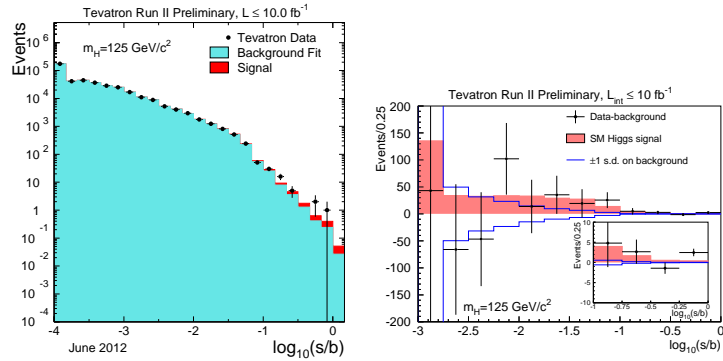


Figure 3: Distribution of $\log_{10}(s/b)$ (left) for the data from all contributing Higgs boson search channels from CDF and D0 with $m_H = 125 \text{ GeV}/c^2$. The data are shown with points and the expected signal is shown red stacked on top of the background in blue. The corresponding background-subtracted distribution is on right where the excess of events are consistent with the SM expectation of Higgs boson at $m_H = 125 \text{ GeV}/c^2$.

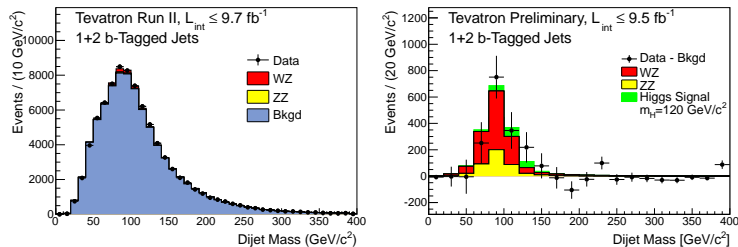


Figure 4: The distribution of the reconstructed dijet mass, before (left) and after (right) background-subtracted, summed over all CDF and D0's channels contributing to the VZ analysis. The fitted VZ and expected SM Higgs ($m_H = 125 \text{ GeV}/c^2$) contributions are also shown with filled histograms.

3 Diboson Searches

To validate our background modeling and search methods, we additionally perform a search for $Z \rightarrow b\bar{b}$ in association with a W or Z boson using the same final states of the SM $H \rightarrow b\bar{b}$ searches. The data sample, reconstruction, background models, uncertainties, and sub-channel divisions are identical to those of the SM Higgs boson search, but the discriminant functions are trained using the signal of $Z \rightarrow b\bar{b}$ instead. The measured cross sections of $WZ + ZZ$ is $3.0 \pm 0.6 \pm 0.7 \text{ pb}$ using the MVA discriminant, which is consistent with the SM prediction of $4.4 \pm 0.3 \text{ pb}$ ¹². The combined dijet-mass distributions before and after background-subtracted for the $WZ + ZZ$ analysis is shown in Figure 4. The signal and the background contributions are fit to the data, and the fitted background is then subtracted. The contribution expected from a SM Higgs signal with $m_H = 125 \text{ GeV}/c^2$ is also included. The diboson cross sections measured by the high mass analysis are also in good agreement with SM predictions¹³.

4 Combined Tevatron Searches

There are no major changes in the analyses since the last update reported at the HCP conference last November¹⁴. Both collaboration have done many cross checks and are focusing on to get the final analyses out for publication. Figure 5 shows the combined limit from each experiment. They have very similar search sensitivities and comparable results.

The ratio of the 95% CL limit on SM Higgs boson production to the SM expected rate is extracted as a function of m_H in the range 90-200 GeV/c^2 , as shown in Figure 6 after combining the CDF and D0 analyses together. We are able to exclude the regions of Higgs boson masses

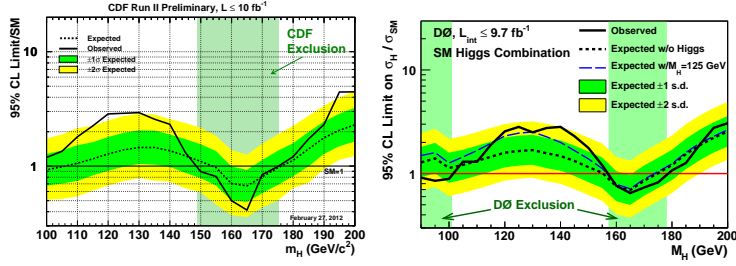


Figure 5: The combined upper limit as a function of the Higgs boson mass between 100 and 200 GeV/c². Solid black: observed limit/SM; Dashed black: median expected limit/SM. Colored bands: ± 1 , 2 sigma distributions around median expected limit from each experiment: CDF (left) and D0 (right).

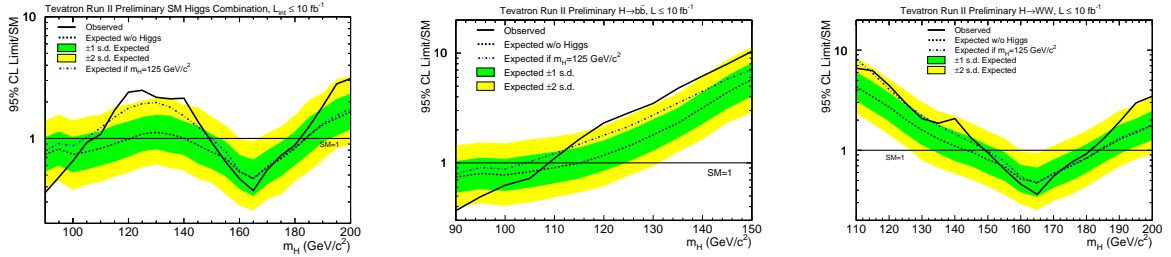


Figure 6: Observed and median expected 95% C.L. upper limits on the production times branching ratio respect to the SM prediction as a function of Higgs boson mass for the combined CDF and D0 searches in all decay channels (left), in the $b\bar{b}$ channels only (center), and in the W^+W^- channels only (right), respectively. The dark- and light- shaded bands indicate the one and two standard deviation probability regions in which the limits are expected to fluctuate in the absence of signal. The blue short-dashed line shows median expected limits assuming the SM Higgs boson is present at $m_H = 125 \text{ GeV}/c^2$.

at 95% CL in 90-107 GeV/c² and 149-182 GeV/c². The expected exclusion regions are 90-121 GeV/c² and 140-184 GeV/c². There is a broad excess observed of events between 115-140 GeV/c². We also separate CDF and D0's searches into combination limits on the $H \rightarrow b\bar{b}$, $H \rightarrow W^+W^-$, $H \rightarrow \gamma\gamma$, and $H \rightarrow \tau^+\tau^-$ decay modes, as shown in Figure 6 and Figure 7.

We quantify the excess by calculating the local p-value for the background-only hypothesis. Figure 8 shows the local p-value as a function of Higgs boson mass where the solid curve is for data and the dash curve is what expected from the SM Higgs boson. At $m_H=125 \text{ GeV}/c^2$, we have a minimum local p-value corresponding to 3 σ standard deviation. The broken line is what expected if a Higgs signal of 125 GeV/c² is present, which has similar shape to the data.

To further check the compatibility with the SM Higgs signal of $m_H=125 \text{ GeV}/c^2$, we compared the log-likelihood-ratio (LLR) after injecting $m_H=125 \text{ GeV}/c^2$ signal into background-only pseudo-experiment, as shown in broken line in Figure 8. The shape seems very similar to what observed in the data and is quite broad due to the fact that MVA is not optimized for mass, but for signal-to-background separation.

The observed excess of m_H from 115 to 140 GeV/c² is driven by an excess of data events with respect to the background predictions in the most sensitive bins of the discriminant distributions. We fit this excess with the signal-plus-background hypothesis and obtain the best-fit signal strength as a function of m_H , shown in Figure 9. The data are consistent with the expectation of a SM Higgs boson in the mass range 115-140 GeV/c². At $m_H = 125 \text{ GeV}/c^2$, the measured signal strength is $1.44^{+0.59}_{-0.56}$.

We also fit to data in separate channels for $H \rightarrow \gamma\gamma$, W^+W^- , $\tau^+\tau^-$, and $b\bar{b}$ for a Higgs mass of 125 GeV/c², as shown in Figure 9. The results are consistent with each other, with the full combination, and with the production of the SM Higgs boson as well. It's worth noting that the best-fit rate cross section for $(\sigma_{WH} + \sigma_{ZH}) \times B(H \rightarrow b\bar{b})$ has measured to be $0.19^{+0.08}_{-0.09}$ pb

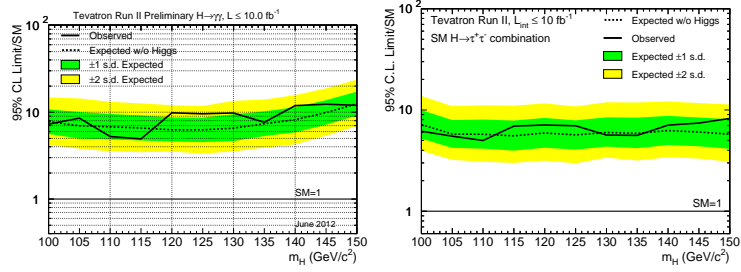


Figure 7: Observed and median expected 95% C.L. upper limits on the production times branching ratio respect to the SM prediction as a function of Higgs boson mass for the combined CDF and D0 searches in the $H \rightarrow \gamma\gamma$ channels (left) and in the $H \rightarrow \tau^+\tau^-$ channels (right), respectively. The dark- and light- shaded bands indicate the one and two standard deviation probability regions in which the limits are expected to fluctuate in the absence of signal.

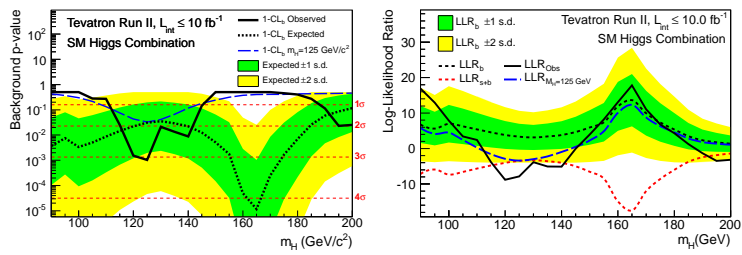


Figure 8: The local background p-value (left) and the log-likelihood ratio LLR (right) are shown as a function of Higgs boson mass for the combined CDF and D0 searches in all channels. The solid lines shows the observed values, the dark short-dash lines show the expected value, and the dark- and light- shaded bands indicate the one and two standard deviation probability regions in which the values are expected to fluctuate.

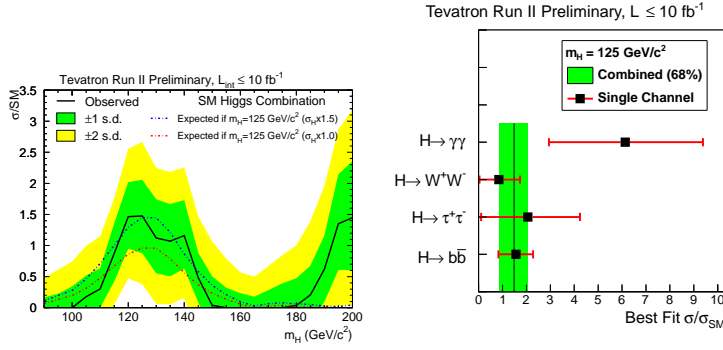


Figure 9: The best-fit signal strength as a function of Higgs boson mass for the combined CDF and D0 searches in all channels (right) and in separate channels for $H \rightarrow \gamma\gamma$, W^+W^- , $\tau^+\tau^-$, and $b\bar{b}$ for a Higgs boson mass of $125 \text{ GeV}/c^2$ (right), respectively. The dark (light) shaded band corresponds to one (two) standard deviation uncertainty on the best-fit value of signal strength with all the channels combined. Also shown on left with blue lines are the median fitted cross sections expected for a SM Higgs boson of $m_H=125 \text{ GeV}/c^2$ with signal strengths of 1 (short-dashed) and 1.5 (long-dashed) times the SM prediction.

for $m_H = 125 \text{ GeV}/c^2$, which is slightly lower, but consistent with the value of $0.23 \pm 0.09 \text{ pb}$ obtained previously⁹ due to the updated $ZH \rightarrow \nu\bar{\nu}b\bar{b}$ analysis from CDF¹⁵.

5 Higgs Boson Properties

In SM, the Higgs boson coupling to other particles is proportional to their mass. Probing its coupling may provide sensitivity to understand what the new particle is, which can be parametrized through coupling factors respect to SM predictions. Most searches at the Tevatron are sensitive to the product of fermion and boson coupling strengths. In the $VH \rightarrow Vb\bar{b}$ channels, the production depends on the coupling of the Higgs boson to the weak vector bosons, while the decay is to fermions. In the $gg \rightarrow H \rightarrow W^+W^-$ channels, the production is dominated by the Higgs boson couplings to fermions via the quark loop process, but the decay is to bosons. We follow the procedures of the LHC Higgs cross section WG¹⁶ and assuming uniform prior for all coupling's. Figure 10 shows the constraining of the custodial symmetry λ_{WZ} , the ratio of Higgs coupling to W boson and Z boson, by fixing all fermion coupling to SM predictions for the combined Tevatron searches for a Higgs mass of $125 \text{ GeV}/c^2$ and two-dimensional constraining of fermion and boson coupling simultaneously by fixing to $\lambda_{WZ} = 1$, respectively. The results are consistent with SM predictions.

6 Conclusion

In conclusion, the final Tevatron results are presented based on full Run II dataset. The Tevatron has achieved SM sensitivity over most of the accessible mass region. We observed a broad excess in the mass range of $115 - 140 \text{ GeV}/c^2$ relative to background-only hypothesis with a local p-value of 3 sigma, consistent with the discovery of a Higgs boson at $125 \text{ GeV}/c^2$. Studies of the couplings at the Tevatron are consistent with SM predictions and are complementary to those performed at LHC.

Acknowledgments

We would like to thank the organizers of the XLVIIIth Rencontres de Moriond electroweak session for a wonderful conference with excellent presentations and the CDF and D0 Collaborations for the results presented.

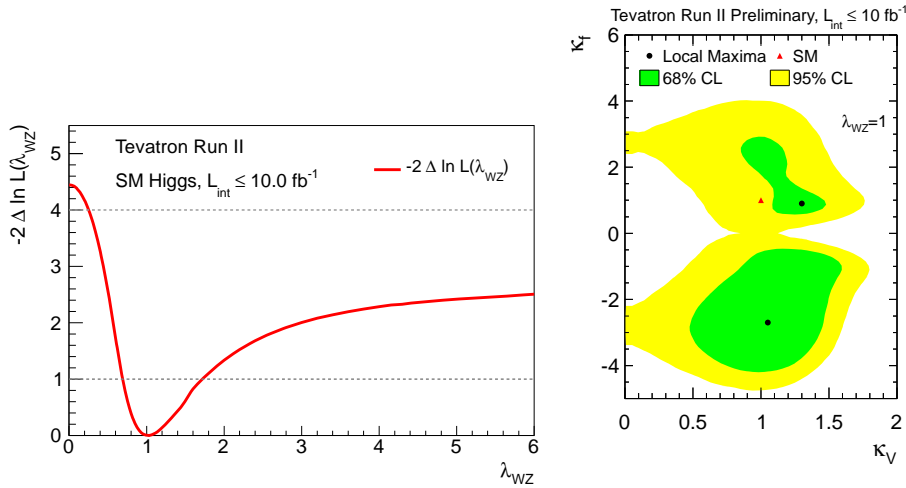


Figure 10: The constraining of the custodial symmetry λ_{WZ} , the ratio of Higgs coupling to W boson and Z boson, by fixing all fermion coupling to SM predictions for the combined Tevatron searches for a Higgs mass of $125 \text{ geV}/c^2$ (left) and two-dimensional constraining of fermion and boson coupling simultaneously by fixing $\lambda_{WZ} = 1$ (right), respectively. The points on right show the best fit from the data with dots, and the dark- and light-shaded regions corresponding to the 68% and 95% CL intervals. The SM prediction is marked with a triangle.

References

1. F. Englert and R. Brout, *Phys. Rev. Lett.* **13**, 321 (1964); P.W. Higgs, *Phys. Rev. Lett.* **13**, 508 (1964); G.S. Guralnik, C.R. Hagen, and T.W.B. Kibble, *Phys. Rev. Lett.* **13**, 585 (1964).
2. The CDF and D0 Collaborations, Higgs Boson Studies at the , arXiv:1303.6346.
3. The LEP Electroweak Working Group, Status of March 2012, <http://lepewwg.web.cern.ch/LEPEWWG/>.
4. The CDF and D0 Collaborations, Combination of the top-quark mass measurements from the Tevatron collider, arXiv:1207.1069.
5. The CDF and D0 Collaborations, 2012 Update of the Combination of CDF and D0 Results for the Mass of the W Boson, arXiv:1204.0042.
6. R. Barate *et al*, *Phys. Lett. B* **565**, 61 (2003).
7. G. Aad *et al*, *Phys. Lett. B* **716**, 1 (2012).
8. S. Chatrchyan *et al*, *Phys. Lett. B* **716**, 30 (2012).
9. T. Aaltonen *et al*, *Phys. Rev. Lett.* **109**, 071804 (2012).
10. TeV4LHC higgs Working Group, Standard Model Higgs cross sections at hadron colliders, <http://maltoni.home.cern.ch/maltoni/TeV4LHC/SM.html>.
11. S. Dittmaier *et al*, arXiv:1201.3084.
12. J.M. Campbell and R.K. Ellis, *Phys. Rev. D* **60**, 113006 (1999).
13. V.M. Abazov *et al*, arXiv:1303.0823.
14. A. Juste, Proceedings of Hadron Collider Physics Symposium 2012, <http://www.icepp.s.u-tokyo.ac.jp/hcp2012/>
15. T. Aaltonen *et al* *Phys. Rev. D* **87**, 052008 (2013).
16. A. David *et al*, arXiv:1209.0040.